LA-UR-01-2833
Approved for public release; distribution is unlimited.

Title: **How Do Numerical Methods Effect the Statistical Details of Richtmyer-Meshkov Instabilities?**

Author(s): W.J. Rider J.R. Kamm, C. Zoldi

Submitted to:

http://lib-www.lanl.gov/la-pubs/00818151.pdf

How Do Numerical Methods Effect the Statistical Details of Richtmyer-Meshkov Instabilities?

W.J. Rider J.R. Kamm, C. Zoldi
Los Alamos National Laboratory, Los Alamos, NM 87545 USA.

1 Introduction

Over the past several years we have presented a less than glowing experimental comparison of hydrodynamic codes with the gas curtain experiment. Here, we discuss the manner in which the various details of the hydrodynamic integration techniques conspire to produce poor results. This also includes some progress in improving the results and agreement with experimental results. Our results are based upon the gas curtain, Richtmyer-Meshkov experiments conducted by Rightley et al. (Rightley et al. 1999) at Los Alamos. We also examine the results of a gas cylinder experiment conducted more recently by Prestridge and Zoldi which includes velocity data obtained via a PIV technique.

Traditionally, the integral width of the mixing layer is used as a yardstick to measure the Richtmyer-Meshkov instability. This is also used when investigating the performance of numerical methods. Our focus has been on the details of the mixing below the integral scale. Because the flow is hydrodynamically unstable, we employ statistical measures in our comparisons. This is built upon a parallel effort by the experimentalists investigating the statistical nature of the mixing induced by shock waves. The principle tools we use to measure the spectral structure of the images of these flows are the fractal dimension and the continuous wavelet spectrum.

The bottom line is that all the higher order methods used to simulate the gas curtain compare poorly with the experimental data when quantified with these spatial statistics. Moreover, the comparisons degrade under mesh refinement. This occurs despite the fact that the the integral scale comparison is acceptable and consistent with the expectations from this class of methods. The most surprising result is that a first-order Godunov method does produce a good comparison relative to the assumed to be higher-order methods. We have examined a broad variety of methodologies associated with the high-order methods to illuminate this problematic result.

In the next section we briefly describe the experiments. In Section the quantitative measures applied to the images are detailed; the results of these analyses are discussed in Section refsec:compare. The consideration of the relation between turbulence models and numerical methods was inspired by these results and is discussed in Section .

2 Experimental Summary

The experiments referred to here have been described by Rightley et al. (Rightley et al. 1999) and references therein. We describe them briefly and focus on aspects that are relevant to our current discussion.

The experimental apparatus is a 5.5 m shock tube with a 75 mm square test section. The driver section is pressurized before the shot, and the rupturing of a polypropylene diaphragm produces a Mach 1.2 planar shock. In the test section, a vertical curtain of SF_6 is injected through a nozzle in the top, and removed through an exhaust plenum at the bottom. Interchangeable nozzles containing different contours impose perturbations on the cross section of the curtain, which has a downward velocity of $\sim$ 10 cm/s.

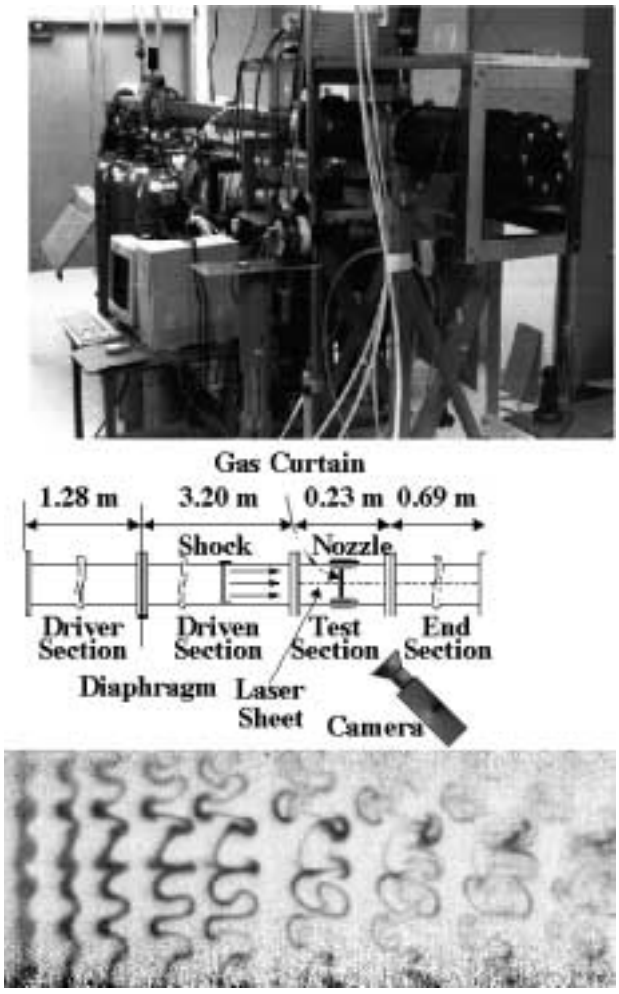

Figure 1. Photograph of the shock tube experimental facility in which the gas curtain experiments are performed. Below the photograph is a diagram of the shock tube and a picture of the raw experimental data obtained.

The evolving flow is imaged by a horizontal laser light sheet. A tracer material consisting of glycol fog (with a typical droplet dimension of 0.5μm) is added to the curtain to greatly improve the dynamic range of the images, which are captured by CCD camera. A detailed discussion of the experimental apparatus, including a discussion of the flow tracking ability of the glycol fog and experimental error analysis, is given by Rightley et al. (Rightley et al. 1999)

One aspect that is central to this work is the fidelity of the experimental images. Many high-speed flow instability experiments do not achieve the image resolution that is obtained with the gas curtain apparatus. This resolution enables a substantive comparison of physical time and space scales with those computed. As a consequence, we seek to make deeper observations regarding the capacity of numerical simulations to model reality.

3 Quantitative Measures of Fluid Mixing

Since pointwise comparisons of the evolving unstable flow are not meaningful, we turn to spectral analysis techniques to quantify the sub-integral scale behavior. In all cases, we use measures with which we can directly compare *quantitatively*, over some range of length scales, experimental observations and computational results. The primary metrics we employ are the fractal dimension and the continuous wavelet spectrum, which we describe briefly.

Fractal analysis has been used extensively to characterize, both theoretically and experimentally, turbulent fluid phenomena (Sreenivasan 1991). This measure, which provides a gauge of the complexity of the flow field, can be directly applied to both experimental observations and computed results. We compute the fractal dimension using the variation method of Dubuc et al. (Dubuc et al. 1989). Additionally, we consider the *local* fractal dimension, which is calculated as the log-log slope of each pair of {scaled length, integrated variation} values; this quantity differs from the *overall* fractal dimension, which is the best fit of the log-log slope over the entire scale range. The outcome of the local method is a plot in which the abscissa is the local length scale and the ordinate is the log-log slope between subsequent pairs of {scaled length, integrated variation} values.

The continuous wavelet transform (CWT) (Farge 1992) is a spectral technique in which a given function or data set is projected onto dilated and translated versions of a basis function, known as the "mother wavelet". The CWT is basically a generalized convolution between the function of interest (e.g., the image of fluid mixing) and a scaled version of the mother wavelet. The mother wavelet we consider is the isotropic Marr or "Mexican hat" wavelet given by $\psi(x,y) = (2 - r^2)\exp(-r^2/2)/\sqrt{2\pi}$, where $r^2 \equiv x^2 + y^2$. Because of specified constraints on the mother wavelet, the CWT provides a quantitative characterization of *local* behavior; this differs from (but is related to) the *global* (or *periodic*) characteristics given by the Fourier transform. Using the CWT results, we compute the *wavelet energy spectrum* (Farge 1992), which is proportional to the integral of the wavelet transform coefficients over all translations. The CWT energy plots show the local wavelet energy intensity as a function of the characteristic wavelet length scale.

4 Comparison of Computations and Experiment

We use the images of the experimental initial conditions to initialize the computations. The images are corrected for noise by using a speckle filter that has a threshold intensity value equal to that of the CCD camera; the denoised images are used in the analysis of the experimental data. The denoised initial condition is smoothed with a Gaussian filter, and then interpolated onto the computational grid, in which the initial computational zone size equals the image pixel size. Reflective boundaries are imposed at the top and bottom of the computational domain.

Our computations are done primarily with the CUERVO hydrocode. CUERVO is a single material code that is primarily used to investigate advanced numerical integration techniques. CUERVO uses unsplit differencing (both spatial and temporal) and an adaptive quadratic two-shock Riemann solver (Rider 1999). There is presently no genuine multidimensional, multimaterial capability. Additionally, other physics can be added to the code without difficulty, a case in point being the diffusive terms (or, e.g., simple turbulence models). We employ this single-material code, as justified by a series of scoping calculations with the multimaterial RAGE code (Baltrusaitis et al. 1996), which indicated no statistically significant difference between single-material and multiple-material simulations of these experiments.

We show in Fig. 2 plots of the SF_6 volume at the initial time (left) and for the flow 400 μs after the initial shock-curtain interaction (right). The corresponding local fractal dimension and CWT spectrum are provided in Fig. 3. The local fractal dimensions indicates that the calculations are more complex at small scales and less complex at large scales relative to the experiment. Similarly, the computed CWT spectra have peaks shifted (but of smaller magnitude) to smaller scales than the experiment, and are deficient in energy at larger scales. Mesh refinement (i.e., running the calculations on finer meshes) did not improve the correspondence, only enhancing the small-scale signatures of the calculations.

We have also run computations using the same initial conditions on identical and finer computational mesh with several other codes. Among the characteristics of these various codes are adaptive mesh refinement (AMR) (Baltrusaitis et al. 1996), various integration methods, including positive methods (Lax et al. 1998), WENO schemes (Shu & Jiang 1997), the HLLE Riemann solver (HLL 1983), and discontinuous Galerkin methods (Cockburn & Shu 1998). None of these methods, which are all nominally at least second order, gave

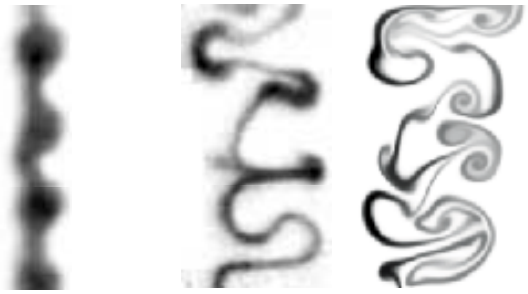

Figure 2. SF_6 volume fraction at the initial time (left) and for the evolved flow at 400 μs (right), with the experimental image on the left and the second-order Cuervo result on the right.

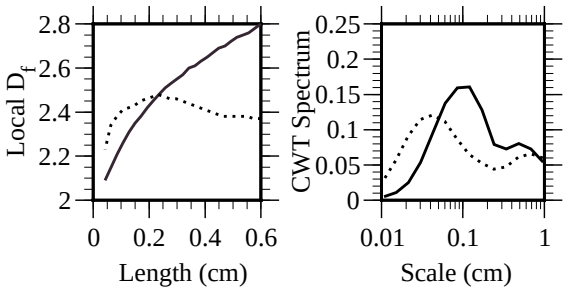

Figure 3. Local fractal dimension (left) and CWT spectrum (right) for the images of Fig. 2 as functions of scale. The experimental result is a solid line, and the computed result is a dotted line.

a notable improvement in the spectral signatures of the calculation relative to the experiment.

From these results, we hypothesized that some aspect of the high-resolution methods may be introducing additional high-frequency information in the simulations. Therefore, we performed a series of calculations in which the integrator was first-order accurate. We provide in Fig. 4 images of the experiment and first-order computation at 400 μs; Fig. 5 shows corresponding fractal and CWT spectra. The agreement of spectral shape and amplitude for both the local fractal dimension and CWT spectra is notably better for the first-order calculations than for the higher order methods.

5 Numerical Methods as Turbulence Models

We explicitly focus on the hyperbolic part of the fluid dynamic equations (i.e., the nonlinear transport terms that are responsible for turbulence). The nonlinear interactions induced by these terms cause scale-to-scale transfer of energy, resulting ultimately in entropy production by viscosity. At large scales in the inertial range, the flow behaves (nearly) independently of viscosity. In addition, important energy transfers known as *backscatter* move energy from small scales toward larger scales. This process is not represented in those turbulence models that are

Figure 4. SF_6 volume fraction at 400 μs for the experimental image (left) and the first-order Cuervo result (right).

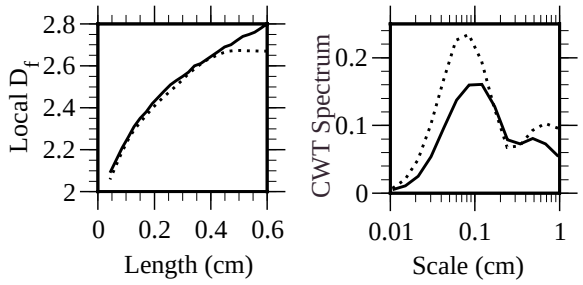

Figure 5. Local fractal dimension (left) and CWT spectrum (right) for the images of Fig. 4 as functions of scale. The experimental result is a solid line, and the computed result is a dotted line.

purely dissipative. Conversely, this effect is naturally present in the hyperbolic terms. We will operate under the assumptions of large eddy simulation (LES). For example, we assume the numerical solution resolves the energy-containing range of the flow, i.e., that the grid scale is in the inertial range. The book by Pope (Pope 2000) describes the state-of-the-art in turbulence modeling.

It is useful to contrast certain aspects of turbulence modeling with numerical methods for hyperbolic PDEs. One computes hyperbolic PDEs with two competing criteria in mind: a desire for high accuracy coupled with guards against catastrophic failure due to nonlinear wave steepening or unresolved features. Nonlinear mechanisms guard the method from such catastrophic failures by triggering entropy producing mechanisms that safeguard the calculation when the need arises. It is the dominance of the transport (hyperbolic) terms that leads to turbulence. As hyperbolic terms become more important, the problems become more sensitive to initial conditions in the presence of hydrodynamic instability. In compressible flows, the scale-changing phenomena cause wave steepening and shock waves. Dissipation acts to regularize the flow, thereby allowing shock propagation to proceed physically even while it is unresolved on the computational mesh.

As motivation for considering the utility of shock-capturing methods for turbulence, we consider the following similarity among many theoretical models.

During the early 1940s, similar forms of dissipation were derived on both sides of the Atlantic. Kolmogorov (Kolmogorov 1962) defined a dissipation of kinetic energy that was independent of the coefficient of viscosity. In this form, the average time-rate-of-change of dissipation of kinetic energy (K) is given as

$$\langle K_t \rangle \; \mathcal{L} = \frac{5}{4} \left\langle (\Delta u)^3 \right\rangle . \qquad (1)$$

In homogeneous, isotropic turbulence, this term is proportional to the average velocity difference at a length scale, $\mathcal{L}$, cubed. In 1942, Bethe (citecpcm) derived the dissipation rate due to the passage of a shock wave. This rate depends on the curvature of the isentrope, $\mathcal{G}$, and on the cube of the jump of dependent variables across the shock:

$$T \Delta S = \frac{\mathcal{G}}{12} \left(\Delta V \right)^3 . \qquad (2)$$

Bethe defined this jump in terms of specific volume, V, but this can be restated in terms of velocity by applying the Rankine-Hugoniot conditions, $s \Delta V = -\Delta u$, where s is the shock speed. Both of these results are analytic. In each of these cases, the flow experiences an intrinsic asymmetry since the dissipative forces arise predominantly where velocity gradients are negative (i.e., compressive).

Eyink (Eyink 1995) studied a conjecture by Kraichnan that the dissipation of kinetic energy as defined by the Kolmogorov similarity is both local as well as integral in nature (by definition, the shock dissipation is local). It is this idea, viz., the existence of a finite rate of dissipation independent of viscosity with an inherently local nature, that we seek to exploit. These regularizations are the essence of the physical conditions that numerical methods must reproduce correctly. Modern high-resolution methods have an effective subgrid model that is inherently local. In addition, the algebraic form of the nonoscillatory methods has a great deal in common with scale-similarity forms of LES subgrid models coupled with a nonlinear eddy viscosity. This creates a coherent tie between the modern nonoscillatory shock capturing methods and LES subgrid models.

We will describe the similarities between modern numerical methods and LES models. One can show that control volume differencing can be viewed as a form of implicit spatial filtering. This is a direct consequence of calculating mean, cell-averaged values. Furthermore, control volume differencing naturally produces terms that are analogous to scale-similarity subgrid models. We will show how numerical flux limiters can act like a dynamic, self-adjusting model, modifying the numerical viscosity to produce a nonlinear eddy viscosity familiar to the turbulence modeler. Overall, a broad class of modern numerical methods can be viewed as dynamic mixed LES models. This analogy is predicated upon the structure of the modified equations for this class of methods (Margolin et al. 2001).

To assess the similarities of high-resolution methods with LES models, we will focus on the numerical interfacial flux F, constructed in these methods as

$$F_{LR} = \frac{1}{2} \left(F_L + F_R \right) - \frac{1}{2} \left| A \right| \left(U_R - U_L \right) , \qquad (3)$$

where L and R denote the left and right states in the Riemann solution, U is the array of flow variables, and A is the flux Jacobian. The absolute value of A can be found via an eigendecomposition, $A = \mathcal{R} \left| \lambda \right| \mathcal{L}$, where these are the right eigenvectors, eigenvalues and left eigenvectors of A. The states can be accessed via interpolation from cell centered to the edges. Thus, the states are extrapolated to a common cell edge from adjacent cell centers. The flux can be generally decomposed into terms that are hyperbolic and that are dissipative in nature. The portion that is the sum of the local contributions (the mean flux) is hyperbolic, while those proportional to the difference in the variables is dissipative with a magnitude proportional to the coefficient of numerical viscosity.

These states can be further decomposed in the spirit of a Reynolds decomposition, $u + u'$, where the u' is defined by a nonlinear interpolation function. This gradient is modified by a nonlinear limiter, $u = \bar{u} + (x - x_0) \phi \; \partial u / \partial x$, where ϕ is the limiter, which is a function of the local data. These expansions are carried out differently in each computational cell, thereby making the effective modeling inherently local. In modern methods, these limiters are nonlinear "switches" that are used to preserve monotonicity (see Leveque (Leveque 1990) for a review). The preservation of monotonicity through nonlinear differencing (e.g., limiters) was developed in parallel by several researchers in the early 1970s. These approaches originated in the work of Godunov, who proved that a linear method cannot be simultaneously second-order accurate and monotone, and culminated in the FCT and MUSCL. TVD methods provided a mathematical structure that extended earlier heuristic and geometric notions. More recently, a number of other nonoscillatory methods have been developed. We will extend these concepts to include continuum and turbulent properties previously not considered explicitly in the design of those methods.

The truncation error of a method is an important indicator of its performance. Here we advocate a more active point of view: that one should *design* the nonlinear truncation error to better mimic turbulence modeling. The "modified equation" is the PDE that a numerical method effectively solves, including leading-order estimates of the truncation error. In this sense, the modified equation describes specific *continuum* properties of a scheme. While such properties are important, one must also remain mindful of important *discrete* properties to maintain such as preservation of monotonicity or positivity. The limiters, ϕ, can be cast in a differential form resulting from their modified equations. In the case of a sign-preserving limiter, the form is $1 - C \Delta x |u_x / u|$ and for a monotone (minmod) limiter it $1 - C \Delta x |u_{xx} / u_x|$. The sign-preserving limiter produces a form for the viscosity that is similar to Smagorinsky's nonlinear viscosity. We can show that these forms play an essential role in the effective dissipation of a scheme

and as well as acting as a trigger for a dynamic dissipative scheme. Also, we can see the implicit correspondence between some limiter forms to dynamic LES models in which the viscosity is adjusted locally based on whether the flow exhibits a similar structure at adjacent length scales. The limiters provide additional utility by comparing several local estimates of a derivative. If these estimates are close enough in magnitude, the flow is treated as being resolved, allowing the method to detect laminar flow.

The first numerical method to employ regularization was artificial viscosity, invented by von Neumann and Richtmyer (von Neumann 1950). There is a close connection of the differential forms used in the von Neumann-Richtmyer artificial viscosity and the Smagorinsky eddy viscosity often used in LES. Indeed, this connection is more explicit than is commonly appreciated, as the original motivation for Smagorinsky's viscosity was to use a nonlinear von Neumann-Richtmyer viscosity to stabilize calculations (Smagorinsky). These two forms of dissipation differ chiefly in the detailed form of their nonlinear terms in multiple dimensions. Further similarities exist with the form of the third-order terms found in the Camassa-Holm equations (Camassa & Holm 1993). Because the Camassa-Holm equations imply a dissipation that results from time-averaging determined by dynamical theory, there is a strong connection between the entropy production and the proper nonlinear dissipative form. Such observations suggest that these methods all share common dynamical mechanisms for producing entropy, leading to their similar scaling of physical solutions.

Nonoscillatory methods are used to simulate a broad variety of physical processes including unstable flows that are dominated by vorticity leading to turbulence, and the mixing of materials (Boris 1989). The properties of such methods appear to infuse the simulations with many of the characteristics of turbulent flows. At present, this capability is largely observational, without significant theoretical support. Nonetheless, these methods appear to achieve many of the properties of subgrid models (Boris 1989, Margolin et. al. 1998) used in LES (Eyink 1995, Pope 2000). The principal element missing in the use of this broad class of methods is the theoretical framework to justify their observed utility in simulations of turbulent flow. Perhaps more importantly, these methods are often necessary to ensure a stable computation. Ultimately, this research is an acknowledgement that physical phenomena, associated models and their numerical solution are intertwined and should be considered together. At present, such an approach is lacking in simulation where models are developed independently, under the assumption of an error-free solution.

Given this development we attempt to develop a dynamic turbulence model, where the numerical dissipation will turn off whenever the flow is locally resolved. This is common with limiters where a high-order method is chosen whenever the flow is smooth enough. A standard example is the van Leer limiter, where given left and right slopes, $\partial_l u$ and $\partial_r u$. The high-order slope is $\partial_c u = \frac{1}{2}(\partial_l u + \partial_r u)$, the limiter reads, $\partial u = S \max[0, \min(2S\partial_l u, 2S\partial_r u, |\partial_c u|)]$ with $S = \text{sign}(\partial_c u)$. Here, as long as all the gradient estimates have the same sign and the centered gradient is not larger than twice either of the one-sided estimates, the centered gradient is chosen.

Given that this limiter provides a modified equation form like $1 - \Delta x\,|u_{xx}/u_x|$, we will design a limiter that produces a Smagorinsky dissipation, $1 - \Delta x\,|u_x/u|$. In order to accomplish this end, the limiter should switch off when the flow is resolved. This is determined by the switching function, $\psi_{i,j} = 1 - (\max u_{i,j} - \min u_{i,j}) / |\min u_{i,j} + \max u_{i,j}|$. The overall limiter is then chosen to give the dynamic feature, $\partial u = \min(1, 2\psi_{i,j})\,\partial_c u$. Thus, when the switch ψ is greater than $\frac{1}{2}$ in value, the centered gradient will be chosen to approximate, ∂u.

We now examine the performance of this limiter when used to replace our standard monotone limiter in simulating the gas curtain. Our results are computed using a modified version of our Cuervo code. Our results are shown in Figure 6 and statistically in Figure 7. In a statistical sense the results with the dynamic Smagorinsky limiter are better than the standard method.

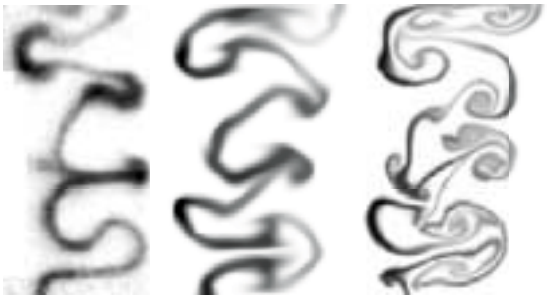

Figure 6. SF_6 volume fraction at 400 μs for the experimental image (left) the dynamic Smagorinsky Cuervo result (center), the second-order standard MUSCL-type scheme (right).

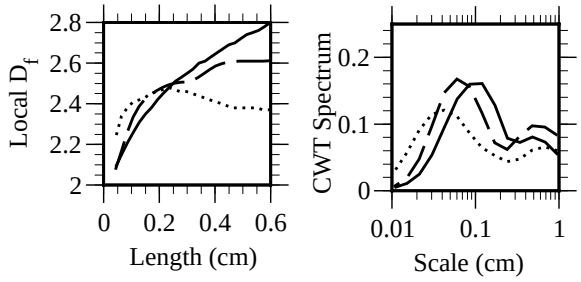

Figure 7. Local fractal dimension (left) and CWT spectrum (right) for the images of Fig. 6 as functions of scale. The experimental result is a solid line, and the computed result is a dotted line.

6 Summary

We have examined the gas curtain Richtmyer-Meshkov experiment of (Rightley et al. 1999) and numerical simulations of that experiment using a scale-dependent fractal dimension measure and the continuous wavelet transform spectrum. We find significant variations in the spectral signatures of different numerical methods on the gas curtain simulations. Different high-resolution shock capturing schemes exhibit quantitatively similar behavior; these results, however, vary from first-order results, which are closer to the experiment, both qualitatively and quantitatively, than those of the (ostensibly "better") high resolution methods. These results are not meant to imply that high-order methods should not be used; rather, our viewpoint is that the high-order methods at present are not suitable for calculations of these experiments and must be modified to improve results.

We speculate that some aspects of high-resolution methods for multidimensional compressible flow may be undermining the statistical scaling in the gas-curtain Richtmyer-Meshkov simulations. Examination of the modified equations associated with high-resolution methods as applied to the gas-dynamic equations has yielded the enticing hint that characteristics implicit in these methods may mimic certain aspects of turbulent flow modeling (Margolin et al. 2001). The implicit turbulent modeling aspects of high-resolution methods may provide a fruitful avenue by which to gain understanding of the simulation of unstable flows of compressible fluids.

Lastly, we observe that experiments with high fidelity diagnostics were critical to uncovering these issues. We would be delighted to have flow diagnostics of even higher spatial resolution. We argue that quantitative "apples to apples" comparisons of experimental data with numerical results provide the most meaningful and compelling measure of the capabilities of numerical simulation.

Acknowledgement

This work is available as Los Alamos National Laboratory report LA–UR-01–2833, and was performed at Los Alamos National Laboratory, which is operated by the University of California for the United States Department of Energy under contract W-7405-ENG-36.

References

R. M. Baltrusaitis, M. L. Gittings, R. P. Weaver, R. F. Benjamin & J. M. Budzinski (1996), Simulation of shock generated instabilities, *Phys. Fluids*, **8**:2471–2493.

H. A. Bethe (1998), On the Theory of Shock Waves for An Arbitrary Equation of State, in *Classic Papers in Shock Compression Science*, J.N. Johnson & R. Cheret (eds.), Springer-Verlag, Berlin.

J. P. Boris (1989), in *Whither Turbulence? Turbulence at the Crossroads*, J. L. Lumley (ed.), Springer-Verlag, Berlin.

R. Camassa and D.D. Holm (1993), An integrable shallow-water equation with peaked solitons, *Phys. Rev. Lett.*, **71**:1661–1664.

B. Cockburn and C.-W. Shu (1998), The Runge-Kutta discontinuous Galerkin method for conservation laws V : Multidimensional systems, *J. Comp. Phys.*, **141**: 199–224.

B. Dubuc, S. W. Zucker, C. Tricot, J. F. Quiniou & D. Wehbi (1989), Evaluating the fractal dimension of surfaces, *Proc. Roy. Soc. Lond. A*, **425**:113–127.

G. Eyink (1995), Local energy flux and the refined similarity hypothesis, *J. Stat. Phys.*, **78**:335–351.

M. Farge (1992), Wavelet transforms and their applications to turbulence, *Ann. Rev. Fluid Mech.* **24**:395–457.

U. Frisch (1996), *Turbulence: The Legacy of A.N. Kolmogorov,* Cambridge University Press, Cambridge 57–71 and 89–91.

A. Harten, P. D. Lax and B. van Leer (1983), On Upstream Differencing and Godunov-Type Schemes for Hyperbolic Conservation Laws, *SIAM Review*, **25**: 35–61.

A. Kolmogorov (1962), A refinement of previous hypotheses concerning the local structure of turbulence in a viscous incompressible fluid at high Reynolds number, *J. Fluid Mech.*, **13**:82–85.

P. D. Lax & X.-D. Liu (1998), Solution of two-dimensional Riemann problems of gas dynamics by positive schemes, *SIAM J. Sci. Comput.* **19**(2):319–340.

R. J. Leveque (1990), *Numerical Methods for Conservation Laws*, Birkhauser-Verlag, Basel.

L. G. Margolin, P. K. Smolarkiewicz & Z. Sorbjan (1998), Large eddy simulations of convective boundary layers using nonoscillatory differencing, *Physica D*, **133**:390–397.

L. G. Margolin & W. J. Rider (2001), *A Rationale for Implicit Turbulence Modeling*, ECCOMAS September 2001, Submitted to the International Journal for Numerical Methods in Fluids, also see LA-UR-01-793.

S. B. Pope (2000), *Turbulent Flows*, Cambridge University Press, Cambridge.

W. J. Rider (1999), An Adaptive Riemann Solver Using a Two-Shock Approximation, *Comp. Fluids*, **28**:741–777.

P. M. Rightley, P. Vorobieff, R. Martin & R. F. Benjamin (1999), Experimental-observations of the mixing transition in a shock-accelerated gas curtain, *Phys. Fluids*, **11**:186–200.

C.-W. Shu and G. S. Jiang (1996), Efficient implementation of weighted ENO schemes, *J. Comp. Phys.*, **126**: 202–228.

J. Smagorinsky (1983), The Beginnings of Numerical Weather Prediction and General Circulation Modeling: Early Recollections, *Advances in Geophysics*, **25**: 3–37.

K. R. Sreenivasan (1991), Fractals and multifractals in fluid turbulence, *Ann. Rev. Fluid Mech.*, **23**:539–600.

J. von Neumann & R. D. Richtmyer (1950), A method for the numerical calculation of hydrodynamic shocks, *J. Appl. Phys.*, **21**:232-237.